Available online at www.sciencedirect.com
SCIENCE DIRECT
materials letters
Materials Letters 59 (2005) 3325 – 3329
www.elsevier.com/locate/matlet

Effect of residual shear bands on serrated flow in a metallic glass

Chunguang Tang [a], Yi Li [a], Kaiyang Zeng [b,*]

[a]Department of Materials Science, National University of Singapore, 10, Lower Kent Ridge Crescent, 119620, Singapore
[b]Department of Mechanical Engineering, National University of Singapore, 9 Engineering Drive 1, 117576, Singapore

Received 16 December 2004; accepted 26 May 2005
Available online 16 June 2005

Abstract

This work studies the effects of the shear bands on serrated flow of the metallic glass Zr–5Ti–17.9Cu–14.6Ni–10Al using nanoindentation technique and scanning electronic microscopy (SEM). It was observed that the nanoindentation load–displacement (P–h) curves are serrated when the nanoindents were made within the region had pre-introduced shear bands from a spherical indentation made with higher load in the specimen. The results support the earlier observation and assumption that the pre-introduced shear bands intersect with the new shear bands induced by nanoindentations, leading to less pile-up around the nanoindentation impressions. This result is discussed with possible mechanisms of the plastic deformation of the metallic glass materials.

Keywords: Metallic glass; Shear band; Serration; Nanoindentation

1. Introduction

Plastic strains in bulk metallic glass (BMG) are usually carried by narrow shear bands, in consequences of shear bonds nucleation and propagation, discrete bursts, or serrated plastic flow is usually observed. The importance of the shear bands in plastic deformation of BMGs has been studied extensively. The interception of the shear bands can contribute substantially to the increases of tensile ductility of the BMGs. For example, Takayama [1] investigated the drawing behavior of $Pd_{77.5}Cu_6Si_{16.5}$ amorphous alloy wires and found that two families of deformation markings (shear bands) appeared on the specimen surface with rather regular intersections between them. On the peripheral surfaces of drawn metallic glass wires, he found that one shear band often terminated at another shear band. Based on this fact, he suggested that a plastically pre-deformed area in metallic glasses could cause an obstacle to an intersecting shear band system. He proposed that such intersection of shear bands in metallic glasses could contribute to work hardening of the material, which could suppress the catastrophic failure during drawing. In fact, his tensile tests indicated that, compared to un-drawn wires, drawn metallic glass wires possessed slightly higher fracture stress and substantially larger plastic strain.

Recently, Schuh et al. investigated serrated flow during nanoindentation on several metallic glass materials [2–4]. It was found that at lower loading rates, the nanoindentation load–displacement curves (P–h curves) were serrated, while at high loading rates, the curves were quite smooth. At lower loading rates, the figures of strain rate versus displacement showed certain peaks, corresponding to the serrations (also called pop-in) on the P–h curves. They proposed [2] that at very low loading rates, few shear bands or even a single shear band could rapidly accommodate the applied strain and thus serrated P–h curves occurred; at high loading rates, many shear bands were required at every instant in order to accommodate the applied strain and thus continuous plastic deformations or smooth P–h curves occurred. This proposal is supported by the observations of Jiang and Atzmon [5] who have conducted Berkovich nanoindentations on metallic glass $Al_{90}Fe_5Gd_5$ at different loading rates and found that: (i) at high loading rates, the P–h curve was smooth and many shear bands with small

* Corresponding author.
E-mail address: mpezk@nus.edu.sg (K. Zeng).

0167-577X/$ - see front matter © 2005 Elsevier B.V. All rights reserved.
doi:10.1016/j.matlet.2005.05.066

spacing were formed around the indent; (ii) at low loading rates, the $P-h$ curve was serrated and only a few shear bands with large spacing were formed around the indent. By now, almost all of these nano-indentation work is concentrated on the loading rate effects, in which, of course, is an important factor which affects the plastic deformation of the BMGs.

During our previous work of spherical indentation on bulk metallic glass Zr–5Ti–17.9Cu–14.6Ni–10Al (wt.%) (vit105), we found that shear bands formed in the free surface around the indentation impression [6]. Furthermore, we performed Berkovich nanoindentations around the spherical indentation impression and found that the material near the spherical indentation impression showed apparent lower hardness than that of the material far away from the spherical indentation impression. Further investigation by Atomic Force Microscopy (AFM) and Scanning Electron Microscopy (SEM) revealed that the residual contact area of the nanoindentation sites located near the spherical indentation impression was large, accompanied by little pile-up and few shear bands around them, whereas the nano-indentation sites located far away from the spherical indentation impression was smaller, but with substantial pile-up and more shear bands around. We attributed that the hardness differences mainly arise from the pile-up, which would result in underestimated contact area and hence overestimated hardness.

It is well known that at room temperature, the plastic strain of metallic glasses is confined in the inhomogeneous shear bands and out of the shear bands the material is only elastically deformed [7]. Based on this fact, we believe what happened is that: (i) near the spherical indentation impression, the pre-introduced shear bands by spherical indentation interacted with the new shear bands produced by Berkovich nanoindentation and suppress the latter, leading to less pile-up around the nanoindentations; (ii) far away from the spherical indentation impression, the shear bands induced by nanoindentations are not suppressed by the pre-introduced shear bands and thus are able to produce pronounced pile-up around the nanoindentations. In this short report, we will report some further experimental results of the plastic flow during nanoindentation on the same metallic glass material. Our focus is on the influences of the pre-introduced shear bands to the serrated flow behaviour of the BMG material. Our results show that, at the loading rate in which the serration flow is usually not significantly clear under normal conditions, the pre-introduced shear bands will enhance the serrated flow behaviour significantly.

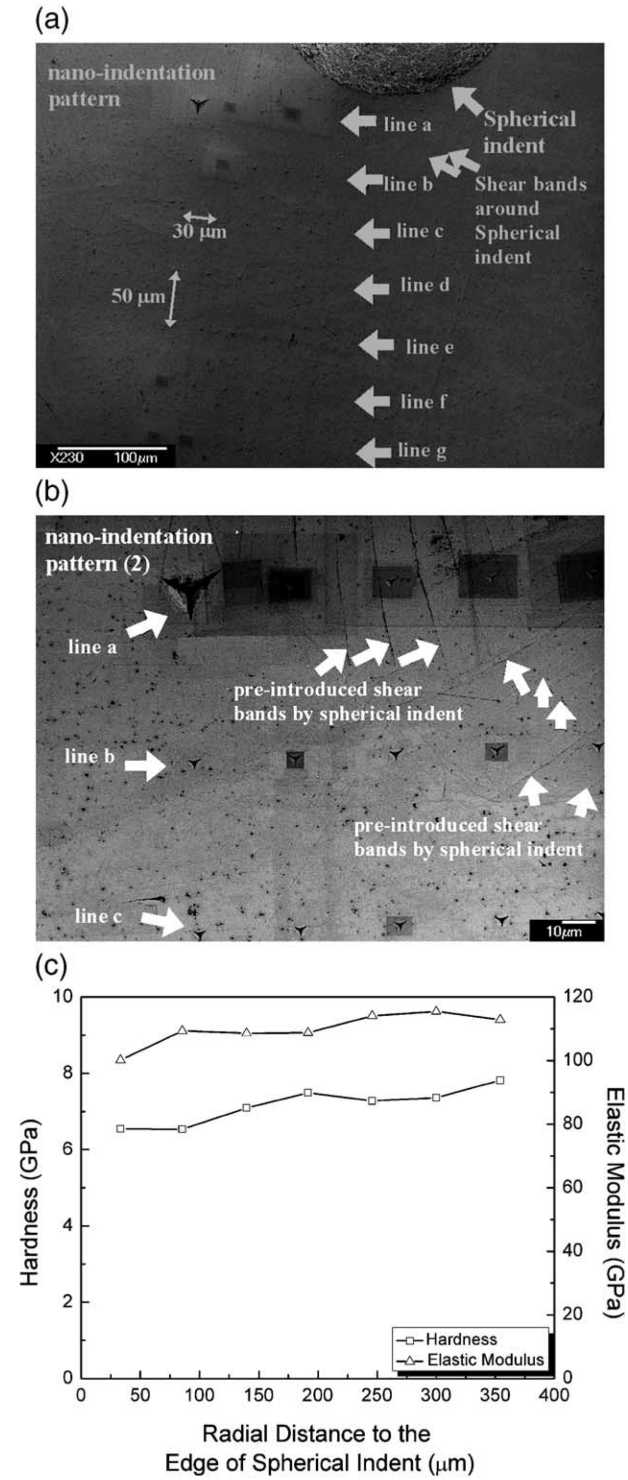

Fig. 1. Patterns of Berkovich nanoindentations around a spherical indentation impression: (a) overall picture (the big indent at the first line is made for surface determination during nanoindentation, and it is therefore excluded from analysis); (b) enlarged picture for the region near the spherical indents; whereas rows (a) and (b) are in the pre-introduced shear bands zone near the spherical indent; rows (f) and (g) are beyond the zone; and (c) the changes of elastic modulus and hardness as function of the distance from the edge of the spherical indents.

2. Experiment

Bulk metallic glass Zr–5Ti–17.9Cu–14.6Ni–10Al (wt.%) (vit105) is prepared by arc melting the pure elements under a Ti-gettered Ar atmosphere, followed by casting into a water-cooled copper mould. The resulting ingot dimensions are $1.6 \times 5 \times 30$ mm^3. X-ray diffraction (Gadds XRD system, Bruker, Germany, with Cu Kα radiation) patterns show no evidence of crystalline phases in the samples.

As-cast samples are mechanically polished to mirror smooth and then indented by a spherical indenter with a nominal radius of 200 μm using Instron Micro-force Tester (Instron Ltd., USA). A spherical indentation impression with radius of 130 μm is therefore produced up to the maximum load of 260 N at displacement rate of 0.1 mm/min.

A series of nanoindentations with Berkovich tip at the maximum load of 40 mN and loading rate of 0.02 mN/s are then performed around the spherical indentation impression using Nanoindenter XP (MTS Cooperation, USA). As shown in Fig. 1(a) for an overall picture, the nanoindentation pattern consists of seven rows with five indents in each row. The nanoindentation impressions in each row are separated by 30 μm distance to avoid interaction of each other and the indentation rows are separated by 50 μm distance. The sampling rate of the nano-indentation is set to be 5 Hz, which is suitable for tracking the details of the indentation process during nanoindentations. The enlarged area including the first 3 rows of nanoindents is shown in Fig. 1(b), it can be clearly seen that lines (a) and (b) are within the region with the pre-introduced shear bands from the spherical indentations (260N for this particular case), whereas line (c) is most likely within the boundaries with and without the pre-introduced shear bands, and the other four lines of nanoindents (d–g) are far away from the spherical indent and therefore represents the material without any influences of the pre-introduced shear bands.

3. Results and discussion

The elastic modulus and hardness around the spherical indents in the radial direction of the spherical indentation are shown in Fig. 1(c). Since the nanoindentations are made in a matrix form, therefore, Fig. 1(c) only represents the changes of the values of elastic modulus and hardness as a function of distance to spherical indent site for the individual indentation sites along one particular radial direction. In this figure, both elastic modulus and hardness showed lower value near the spherical indents, especially the data from the first two to three rows of nanoindentation sites. These results are consistent with previous reported results, in which there is a softer zone around spherical indentation site [6].

At room temperature, metallic glasses deform plastically to show inhomogeneous shear bands. During indentations, the plastic flow builds up and forms pile-up around the indenter. In our experiments, if the pre-introduced shear bands by the spherical indentation impression intersect and suppress the shear bands induced by nanoindentation, less shear bands will operate to accommodate the nanoindentation strain, which should lead to serrated nanoindentation P–h curves, in addition, less pile-up around nanoindentation sites should be expected.

Slow indentation loading rates have been used by Schuh et al. [2–4] in their nano-indentation studies and show that serrated flow and burst at the indentation loading curve could be found under loading rate of 0.02 mN/s or even lower for numbers of BMGs. Therefore, in our current work, the indentation loading rate 0.02 mN/s should start showing some serrated flow and bursts at indentation loading curve for the vt105 material if no other influences existed.

We therefore compared the nanoindentations located in rows (a) and (b) with those in rows (f) and (g) (see Fig. 1(a) for detail). Nanoindentation sites at rows (a) and (b) are near the spherical indentation site and within the regions of shear bands produced by the spherical indentation impression (sees Fig. 1(b)); nanoindentation sites located at rows (f) and (g) are far away from the spherical indentation site and are beyond the zone of pre-introduced shear bands. The loading portions of the load–displacement (P–h) curves for some typical nanoindentations in the four rows are shown in Fig. 2. At the loading rate of 0.02 mN/s, only few small serrations occur on the loading curves of rows (f) and (g). However, the serrations on the loading curves of rows (a) and (b) are more frequent and more pronounced. It should be noticed that the nanoindentation load–displacement curve of row (g) is, in fact, similar to that showed in the work by Schuh and Nieh [2] at the loading rate of 0.04 mN/s.

During nanoindentation with a constant loading rate, the indentation strain rate is defined as $(1/h)(dh/dt)$, where h is displacement and t is time. The strain rate is usually large at the beginning, decreases with displacement at finite depths and approaches a nearly stable value for very large displacements. The strain rates of nanoindentations are plotted as a function of the displacement and shown in Fig. 3. The strain rate peaks, which are found to correlate exactly with the serrations on P–h curves in Fig. 2, reveal the bursts of rapid displacements during the indentations. As Fig. 3 illustrates that the number of strain rate peaks for indentations at rows (a) and (b) are more than that for the row (g); the strain rate peaks for indentations at rows (a) and (b) are also higher and wider. Correspondingly, as shown in the Fig. 2, there are more significant serrations in the P–h curve for rows (a) and (b) in comparison with that of rows (f) and (g). The characteristics of P–h curves for indentations at the last two rows, (f) and (g), are found to be similar.

Figs. 2 and 3 reveal that the plastic flows of the nanoindentations near the spherical indentation impression are more serrated than those far away from it. This is consistent with the

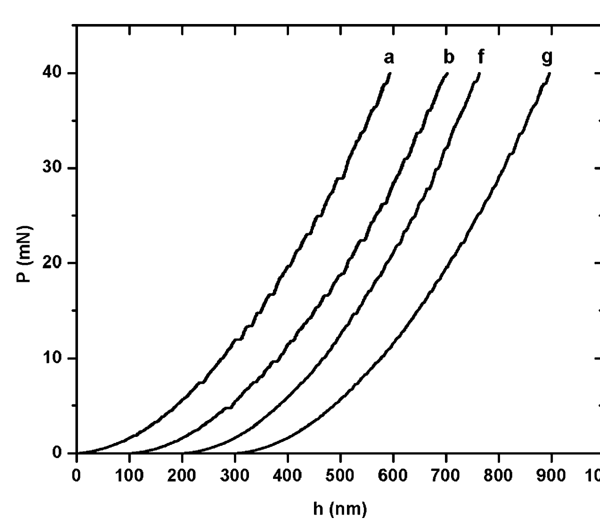

Fig. 2. Typical P–h curves (loading portion) for Berkovich nanoindentations at various distances from the spherical indentation impression: the curves for nanoindentations located in rows (a) and (b) are more serrated than those in rows (f) and (g).

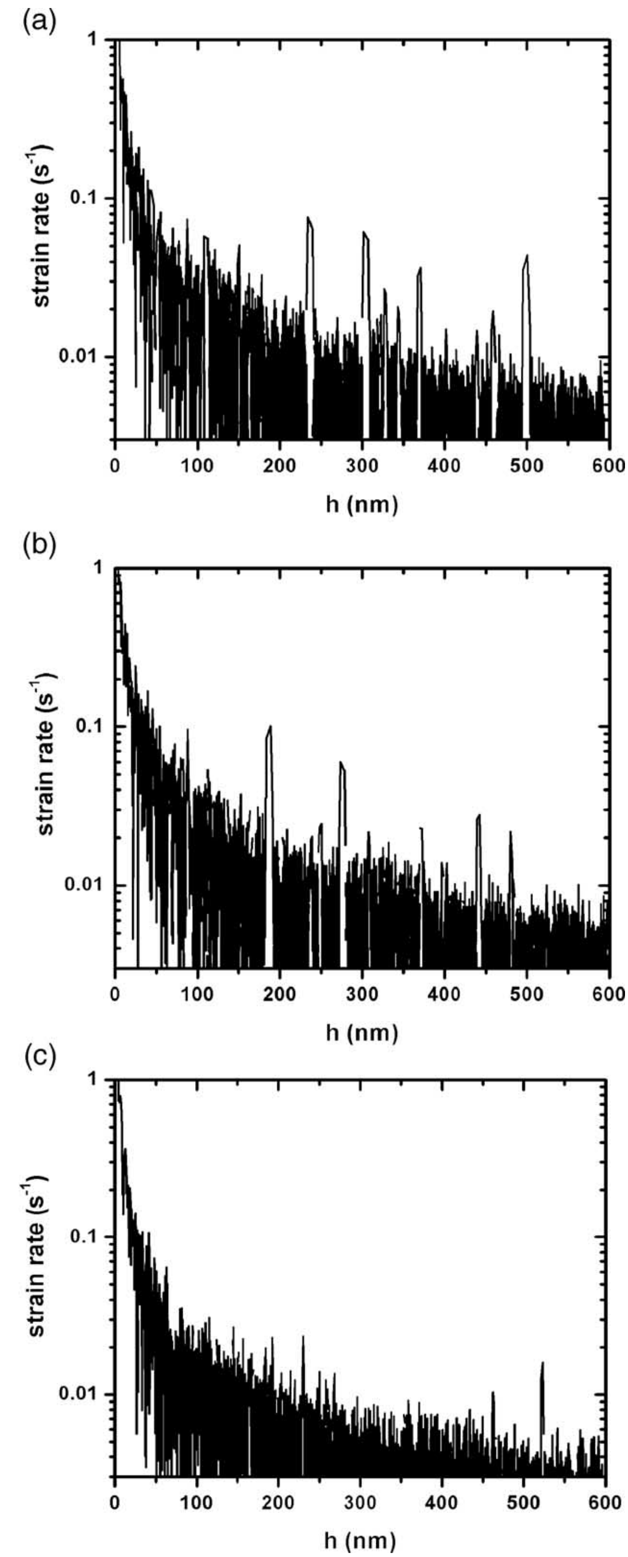

Fig. 3. Strain rate versus displacement plot for the nanoindentation experiments: the strain rate peaks correspond to the serrations on $P-h$ curves. The strain rate peaks in indentation rows (a) and (b) are higher and wider than in row (g).

above assumption that the shear bands around the spherical indentation impression may suppress the shear bands induced by nanoindentations. In fact, our investigations on the shear bands around the nanoindentations also support above conclusion. Only a few shear bands are found on one side or two sides of the nanoindentation impressions that are near the spherical indentation impression (Fig. 4(a–b)); while around the nanoindentation impressions located far away from the spherical indentation impression, pronounced shear bands form on all the three sides, as shown in Fig. 4(c).

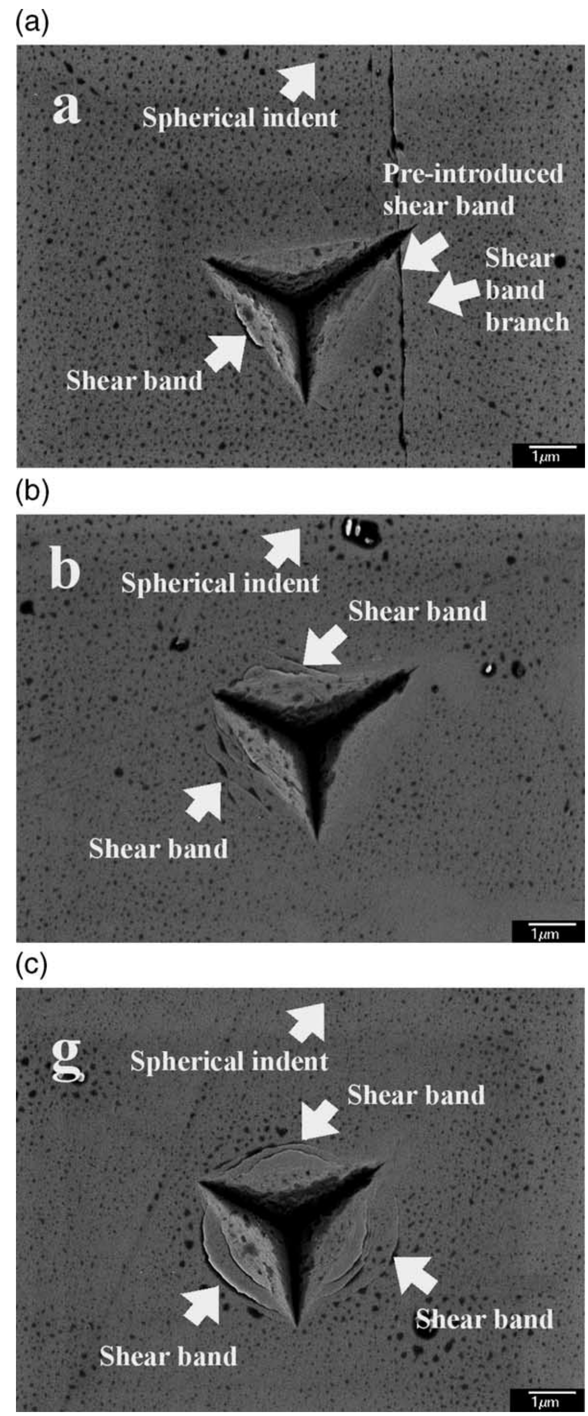

Fig. 4. Shear bands around the Berkovich nanoindentations: the nanoindentations with more serrated $P-h$ curves have less shear bands around them (a–b). The nanoindentations with smoother $P-h$ curves have more shear bands around them (c).

We believe that these results are different from what presented by Hufnagel et al. [8]. Hufnagel et al. have observed that pre-existed shear bands can spawn new "secondary" shear bands [8]. Our results seem to suggest that the pre-existed shear bands (from spherical indent) most likely block the formation of the new shear bands from the nanoindentation sites where they are located at the pre-existing shear band zone, otherwise, it should be observed that there were more shear bands around the nanoindentation sites. However, Fig. 4 reveals that fewer shear bands near the spherical indentation sites, whereas more shear bands formed far away from the spherical indentation sites.

Previously, the serrated indentation load–displacement curves have been observed during slow loading rates indentation [2–4], and lower temperature indentations [9]. This work now adds new observation that the indentation of load–displacement curves can also be serrated by pre-existed shear bands in the metallic glass materials. These results most likely suggested, in additional to the slow loading rates and low temperatures indentation, the formation of individual shear bands is also closely related to the history of the plastic deformation of the metallic glass materials.

4. Summary and conclusions

The present results indicate that, in additional to the loading rate effects, the $P-h$ curve serrations are influenced by the pre-introduced shear bands in the metallic glass material. The pre-introduced shear bands prevent new shear bands formation to accommodate the applied strain, leading to more serrated $P-h$ curves and less shear bands formation around the nanoindentation impressions. This behavior is most likely a special character for the metallic glass materials. A further implication of this work is that, for the metallic glass material, the pre-existed defects, plastic deformation, shear bands and others will significantly affect the behavior of nanoindentation and the properties measured by nanoindentation experiments.

Acknowledgement

The authors would like to acknowledge Institute of Materials Research and Engineering (IMRE), Singapore, for providing experimental facilities for this work.

References

[1] S. Takayama, Mater. Sci. Eng. 38 (1979) 41.
[2] C.A. Schuh, T.G. Nieh, Acta Mater. 51 (2003) 87–99.
[3] C.A. Schuh, T.G. Nieh, Y. Kawamura, J. Mater. Res. 17 (2002) 1651.
[4] T.G. Nieh, C. Schuh, J. Wadsworth, Yi Li, Intermetallics 10 (2002) 1177–1182.
[5] W.H. Jiang, M. Atzmon, J. Mater. Res. 18 (2003) 755.
[6] C. Tang, Y. Li, K. Zeng, Mater. Sci. Eng., A 384 (2004) 215.
[7] F. Spaepen, A.I. Taub, in: F.E. Luborsky (Ed.), Amorphous Metallic Alloys, Butterworth and Co (Publishers) Ltd, 1983, p. 248, Chapter 13.
[8] T.C. Hufnagel, P. El-Deiry, R.P. Vinci, Scr. Mater. 43 (2000) 1071.
[9] C.A. Schuh, A.C. Lund, T.G. Nieh, Acta Mater. 52 (2004) 5879.